Coherent Optical Phase Transfer over a 32-km Fiber with 1 s Instability at 10^{-17}

Seth M. Foreman,[1] Andrew D. Ludlow,[1] Marcio H. G. de Miranda,[1] Jason E. Stalnaker,[2] Scott A. Diddams,[2] and Jun Ye[1]

[1]*JILA, National Institute of Standards and Technology and University of Colorado*
Department of Physics, University of Colorado, Boulder, Colorado 80309-0440, USA
[2]*Time and Frequency Division, MS 847, National Institute of Standards and Technology, Boulder, Colorado 80305, USA*
(Received 1 July 2007; published 9 October 2007)

The phase coherence of an ultrastable optical frequency reference is fully maintained over actively stabilized fiber networks of lengths exceeding 30 km. For a 7-km link installed in an urban environment, the transfer instability is 6×10^{-18} at 1 s. The excess phase noise of 0.15 rad, integrated from 8 mHz to 25 MHz, yields a total timing jitter of 0.085 fs. A 32-km link achieves similar performance. Using frequency combs at each end of the coherent-transfer fiber link, a heterodyne beat between two independent ultrastable lasers, separated by 3.5 km and 163 THz, achieves a 1-Hz linewidth.

Optical atomic clocks with superior stability and accuracy [1,2] demand frequency transfer networks of unprecedented stability for signal distribution, remote synchronization, and intercomparison. Clock signal transfer via optical fiber networks has emerged as a promising solution [3] when phase noise in the long transmission path is effectively canceled [4–6]. In the microwave domain, signals in the form of amplitude modulation of an optical carrier have been transmitted over an 86-km optical fiber, where active stabilization of the fiber's group delay allows a transfer instability of 5×10^{-15} at 1 s and 2×10^{-18} after 1 d [7,8]. However, a direct transfer of the optical carrier itself [9,10] is destined to achieve better stability, with the same advantage of high spectral resolution as the optical clocks. Long-distance coherent transfer of an ultrastable optical carrier signal, along with frequency-comb-based optical coherence distribution over the whole visible spectrum [11,12], permits a variety of applications. They include phase-coherent arrays of radio telescopes [13], precisely synchronized, accelerator-based advanced light sources [14], and precision optical interferometry over a long distance or encircling a large area.

In this Letter, we report experimental implementations of a fully coherent (<1 rad of accumulated optical phase noise) optical-frequency-distribution fiber system spanning tens of kilometers in distance. While 1 s instability of 6×10^{-17} has been achieved in shorter (<1-km) links [12], the 2×10^{-17} instability achieved here on a >10-km link is ~ 100 times lower than previously reported results [10,13]. In a 7-km urban fiber network, the transmission instability is reduced to 6×10^{-18} at 1 s and 1×10^{-19} at 10^5 s, limited by out-of-loop measurements. The integrated phase noise from 8 mHz to 25 MHz is 0.15 rad, representing a coherent optical transfer for time scales much longer than coherence times of the current best optical references. An extended 32-km link employs a transceiver configuration, making an important first step towards the realization of coherent repeaters for unlimited distribution distances. The system achieves similar stabil-

ity performance. Using frequency combs at each end of a third fiber link, we remotely compare two independent Hz-linewidth lasers separated by 3.5 km fiber and spectrally separated by 163 THz. The optical heterodyne beat has a 1-Hz linewidth, limited by the ultrastable lasers.

Figure 1 shows the experimental scheme for phase-coherent optical transfer. To compare the JILA ^{87}Sr optical lattice clock [2] to other optical clocks located at the National Institute of Standards and Technology (NIST) [1,15], we transmit the light from a cw 1064-nm laser,
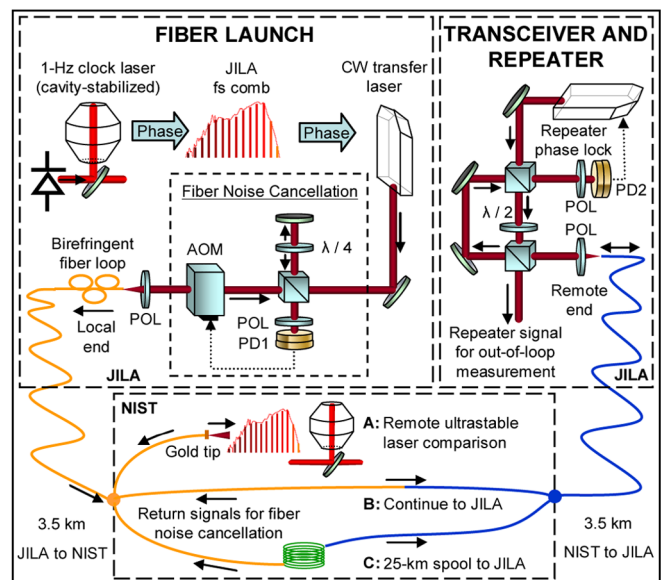

FIG. 1 (color online). Schematic for phase-coherent optical transfer. At the fiber launch the cw transfer laser can be stabilized to a sub-Hz-linewidth clock laser via a fs frequency comb, or left free running. The fiber noise cancellation uses a double-pass AOM as the actuator. Round-trip light used for active noise cancellation comes from either a transceiver laser (transceiver method), or from a partially reflective tip of the fiber (reflection method), at the remote end of the network. Three different fiber networks are characterized.

which is directly measured with Ti:sapphire-based frequency combs serving as the optical clockwork at both locations. For active cancellation of the fiber phase noise, the transfer laser's coherence time must be longer than T_{rt}, the fiber network's round-trip time. Our transfer laser has an intrinsic linewidth of 1 kHz in 1 ms, sufficient for fiber noise cancellation over the 7-km link. For longer fiber links and the remote ultrastable laser comparison, the transfer laser must be stabilized to a sub-Hz-linewidth 698-nm laser [16] serving as the ^{87}Sr clock's local oscillator. A self-referenced, octave-spanning Ti:sapphire laser is used to transfer the clock laser's phase stability across the 148-THz spectral gap to the transfer laser.

For fiber noise cancellation, $\sim$1-mW from the transfer laser is picked off by a polarizing beam splitter (PBS) and detected on photodiode PD1, while $\sim$40 mW is coupled into the fiber (below threshold for stimulated Brillouin scattering) after being frequency shifted by an acousto-optic-modulator (AOM). Light returning from the fiber's remote end accumulates a round-trip phase, again passes through the AOM, and is heterodyned with the local light on PD1. The beat frequency f_{fnc} is used for fiber noise cancellation by phase locking it to a radio-frequency (rf) reference via feedback to the AOM's driving frequency [5,6]. Noise processes that are stationary during T_{rt} (noise bandwidth $<1/2\pi T_{rt}$) are hence precompensated by the AOM, whereas noise at frequencies above this bandwidth is uncanceled. Prescaling of f_{fnc} by a division of 50 is used to give the phase lock enough dynamic range to avoid cycle slips under burst noise.

We test two methods for returning light from the fiber's remote end for noise cancellation. The simpler technique (reflection method) relies on a partially reflective gold coating applied to the flat-polished remote fiber tip. The gold film transmits $\sim$10% of the incident 1064-nm light, used for out-of-loop measurements of the stabilized fiber network, and reflects the rest back to the launch. A more complex technique (transceiver method) uses an angle-polished remote fiber tip and an independent cw laser (transceiver laser) working at the remote end. Light transmitted one way through the fiber network is heterodyned with the transceiver laser on PD2, and the resulting beat signal is used to phase lock the transceiver laser to the transmitted light with a constant frequency offset of 60 MHz. 40 mW of the transceiver light is launched into the fiber network's remote end, to be used for the in-loop fiber noise cancellation at the launch. Additional power from the transceiver laser is used as a repeater signal for out-of-loop measurements of the stabilized fiber network. The reflection method is simple but can be corrupted by unwanted reflections at interconnections along the fiber path. The transceiver method avoids this problem since a different frequency is returned than the input signal. The transceiver method also boosts the power at the remote end and essentially implements a repeater station for a much longer fiber network.

Polarization control for both methods is essential. A set of birefringent fiber loops is used on the input end of the fiber link to adjust the polarization state of the round-trip light to maximize the power of f_{fnc}. The power still fluctuates by $\sim$1 dB at frequencies of a few Hz, and slowly degrades by as much as 5 to 10 dB over the course of 1 d due to time-changing birefringence of the fiber network. Every few hours the loops are adjusted to maximize the strength of f_{fnc}. Another concern is fast time-changing polarization mode dispersion [17]. For the transceiver method a linear polarizer is placed immediately outside the remote end of the fiber to ensure that the incoming polarization used on PD2 is the same as that launched back into the fiber from the transceiver laser. Similarly, a linear polarizer is placed just before the local fiber input. Without the polarizers the fiber noise cancellation does not work, but with them it can be maintained indefinitely with even less sensitivity to the fiber's changing birefringence than the reflection scheme. Rotating the birefringent loops to degrade the power in f_{fnc} by $\sim$10 dB does not affect the performance.

Figure 1, lower panel, shows three different fiber networks configured for various measurements. Two 3.5-km fibers in the Boulder Research and Administrative Network (BRAN) connect JILA with NIST [9]. In setup *A*, only one noise-canceled fiber (reflection method) is used to transmit light for comparing the clock laser at JILA to an independent laser at NIST [18] serving as the Hg$^+$ clock laser. A second octave-spanning frequency comb at NIST spans the 15-THz spectral gap between the transfer laser and the 1126-nm clock laser. A heterodyne beat between the transfer laser and one mode of the frequency comb at NIST characterizes the coherence between the two remotely located clock lasers. In setup *B*, the two 3.5-km fibers are connected together to form a single 7-km (one-way) network. The 7-km fiber has the local and remote ends located on the same table, allowing direct out-of-loop measurement of the transfer system using either the reflection or the transceiver method. In setup *C*, a 25-km spool of SMF-28 fiber is added to the 7-km link. The additional 27-dB loss (each way) makes the reflection method no longer practical, and only the transceiver method is characterized for the 32-km link. No special care is taken to isolate the spool from its environment. For all three setups, the first and last 5-m sections of fiber are single mode for 1064-nm light in an effort to mitigate any effects of time-varying transverse mode dispersion from the slightly multimode BRAN fiber. Attenuation through 7 km of the fiber at 1064 nm is measured as $<$4 dB. All but one interconnection along the 7-km fiber path are fusion spliced to reduce unwanted reflections.

The out-of-loop measurements are made using several different heterodyne beats. We adopt a notation in writing the beat frequencies as $f_{loc,rem}^{(dist)}$, where the first and second subscripts denote light at the local and remote ends, respectively. The superscript denotes the fiber length (km).

Explicitly, the beat between the local transfer laser and the remote light exiting the gold-coated fiber is written as $f_{\text{tfr,tfr}}^{(7)}$. The beat between the local transfer laser and the remote transceiver laser is $f_{\text{tfr,rpt}}^{(7)}$. Similarly, the beat between a mode of the local frequency comb and the remote light exiting the gold-coated fiber is $f_{\text{fs,tfr}}^{(7)}$ while $f_{\text{fs,rpt}}^{(7)}$ denotes the local comb's beat frequency against the remote repeater's light for the 7-km link. For the 32-km link, only $f_{\text{fs,rpt}}^{(32)}$ is characterized. Measurements against the local transfer laser give information only about the fiber link, whereas measurements against the local frequency comb include the phase lock between the transfer laser and frequency comb.

Figure 2 summarizes linewidth characterization results for the various measurements. Figure 2(a) displays the power spectrum of $f_{\text{tfr,tfr}}^{(7)}$ to characterize the 7-km fiber transfer. The uncanceled fiber noise broadens the transferred linewidth to ~1 kHz, while the coherent narrow peak is achieved under active noise cancellation, with a 1.3-kHz servo bandwidth limited by T_{rt} for the 14-km round-trip. Figure 2(c) shows the same data at finer resolution; the energy that spread into a 1-kHz bandwidth by the passive fiber's phase noise is squeezed into the narrow central carrier under active noise cancellation. Figure 2(b) shows $f_{\text{fs,tfr}}^{(7)}$ as a way to additionally characterize the transfer laser's lock to the local frequency comb; the full system operates with a sufficiently small phase noise that a 1-mHz linewidth is recovered. Figure 2(d) shows $f_{\text{fs,rpt}}^{(32)}$ with active

noise cancellation of the 32-km link [narrow carrier in red (or light gray)] and without noise cancellation [flat noise in blue (or gray)]. A narrow coherent feature is present at 0.5-Hz resolution bandwidth, but with less signal-to-noise than for the 7-km transfer because the servo bandwidth is smaller for the longer link. Finally, Fig. 2(e) shows the effective heterodyne beat between the two stable clock lasers at JILA and NIST, linked by the 3.5-km noise-canceled fiber and two independent optical combs. The whole system preserves the full phase coherence of our optical frequency references.

We also directly count the frequencies of the various out-of-loop heterodyne beats. For improved counting resolution, we mix the beat frequencies to 10 kHz using a sufficiently stable rf source. Figure 3 displays the resultant Allan deviations. The open diamonds [in brown (or dark gray)] show typical passive instability for both the 7- and 32-km links. Closed diamonds [in red (or light gray)] are from counting $f_{\text{fs,rpt}}^{(32)}$ to measure the instability of the 32-km transceiver system. Closed circles [in blue (or gray)] use $f_{\text{tfr,tfr}}^{(7)}$ to measure the instability of the 7-km fiber transfer (reflection method). Closed triangles (in black) are the instability of f_{fnc} used for active stabilization of both the 7- and 32-km systems, divided by 2 for a fair comparison against the one-way out-of-loop instabilities. Also shown is a solid black line indicating the effect of 1 rad of accumulated phase noise during the averaging time; the 7-km measurement lies below this level for averaging times $< 3 \times 10^3$ s. The 7-km fiber transfer (reflection method) is locked continuously for 70 h, and for frequency
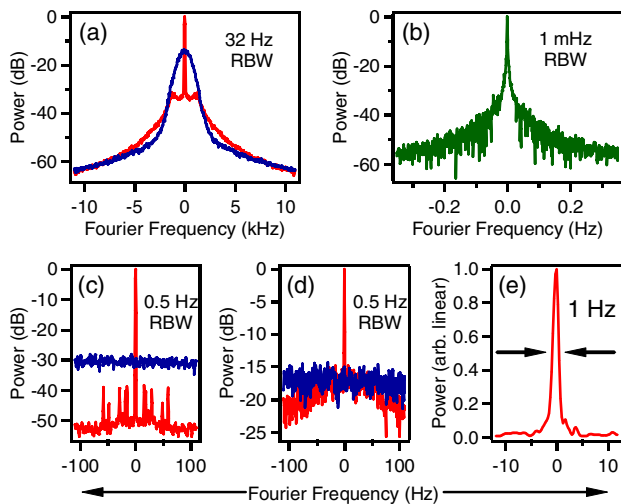

FIG. 2 (color online). Power spectra of various out-of-loop heterodyne beats. (a) $f_{\text{tfr,tfr}}^{(7)}$ characterizes the 7-km transfer only. (b) $f_{\text{fs,tfr}}^{(7)}$ additionally characterizes the transfer laser's lock to the local fs comb. (c) Same as (a), at finer resolution. (d) $f_{\text{fs,rpt}}^{(32)}$ characterizes the 32-km transfer as well as the transfer laser's lock to the local fs comb. (e) The effective beat between independent clock lasers separated by 3.5 km and 163 THz. For (a), (c), and (d) red (or light gray) is for the actively stabilized network and blue (or gray) is for the passive case.
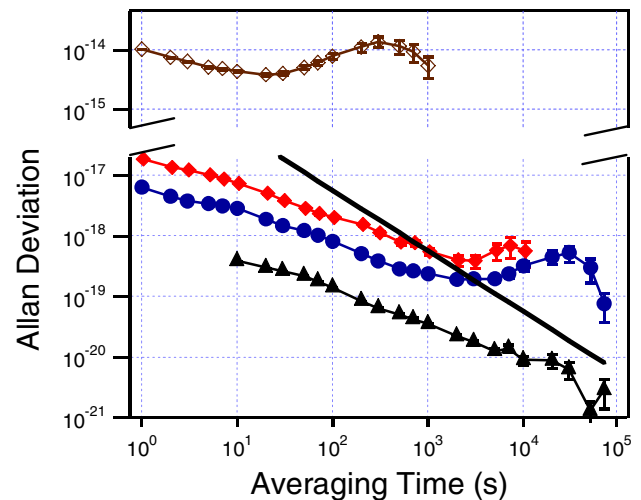

FIG. 3 (color online). Instability of the transfer systems. Open brown (or dark gray) diamonds are typical passive instabilities of the 7- and 32-km fiber links. Closed red (or light gray) diamonds are for the 32-km system, measured by frequency counting $f_{\text{fs,rpt}}^{(32)}$. Closed blue (or gray) circles are for the 7-km fiber transfer, using $f_{\text{tfr,tfr}}^{(7)}$. Black triangles are the instability of f_{fnc} used for in-loop noise cancellation. The solid black line represents 1 rad of accumulated phase noise during the averaging time.
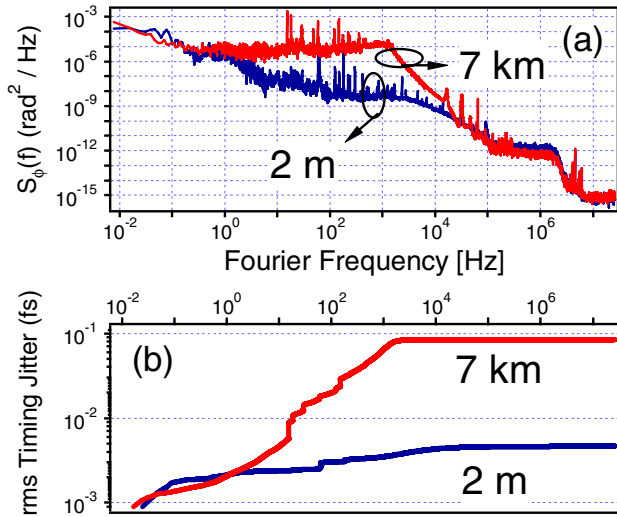
FIG. 4 (color online).   (a) Relative phase-noise spectral density between the local cw transfer laser and light exiting the 7-km fiber link at the remote end. (b) The relative phase noise shown in (a) is integrated and displayed as rms timing jitter, demonstrating 7-km timing transfer with 0.08 fs of jitter integrated from 8 mHz to 25 MHz.

counting $f_{\text{tfr,tfr}}^{(7)}$ with a 10-s gate time, only 0.3% of the counts are outliers. The transfer's accuracy (residual offset from the expected frequency) is 1×10^{-19}, consistent with the long-time-scale instability. The 32-km system is continuously locked for several hours at a time for 14 h (net 85% duty cycle), with a similar amount of outliers. Brief interruptions are caused by the clock laser or the fs frequency comb losing lock, not the transfer or transceiver lasers or the fiber noise cancellation. The accuracy is 5.2×10^{-19}, again consistent with the measured instability from the diurnal temperature fluctuation. To achieve 10^{-17} (10^{-19}) accuracy at 1 s (10^5 s), the various $\sim$100-MHz rf frequency references used for frequency offsets and phase locks must be accurate to $\sim 3 \times 10^{-11}$ (3×10^{-13}).

Both the 7- and 32-km measurements are limited by fluctuations of the out-of-loop optical components. This is confirmed by replacing the 7-km fiber with a 2-m fiber, yielding identical results for time scales up to 10^4 s, even though the passive instability of the 2-m fiber is 100 times smaller than for the 7-km fiber. The system is enclosed in a box to isolate the out-of-loop optics from air currents and acoustic pickup; without the box the 1 s instability rises to several parts in 10^{16}. The excess instability at 2×10^4 s is caused by daily temperature drift of the laboratory. The 32-km transceiver measurement is a factor of 2.5 worse than the 7-km reflection measurement at all averaging times, suggesting that the transceiver measurement's greater out-of-loop complexity sets a higher limiting noise floor. This is confirmed by a comparison of the 7- and 32-km transceiver link instabilities (measured by counting

$f_{\text{tfr,rpt}}^{(7)}$ and $f_{\text{tfr,rpt}}^{(32)}$, respectively) which are identical for averaging times up to 1000 s.

The fiber transfer's coherence is revealed by a direct measurement of the phase noise it introduces. Figure 4(a) shows the phase-noise spectral density $S_\phi(f)$ of the 7-km fiber network [upper curve in red (or light gray)], measured by comparing the phase of $f_{\text{tfr,tfr}}^{(7)}$ against a phase-stable rf reference. The lower curve [in blue (or gray)] shows the same measurement when the 7-km fiber is replaced by the 2-m fiber. For Fourier frequencies between a few Hz and the 1.3-kHz servo bandwidth, the 7-km system's active noise cancellation has insufficient gain to achieve the measurement noise floor represented by the 2-m data. However, below a few Hz the out-of-loop measurement scheme dominates the noise, and is common to both lengths of fiber. The integrated phase noise is displayed as rms timing jitter in Fig. 4(b). Integrated from 8 mHz to 25 MHz, only 0.085 fs of timing jitter is accumulated for the 7-km link, corresponding to 0.15 rad at the optical transfer frequency of 282 THz.

The coherence and stability achieved by this optical transfer scheme permit the most precise optical clock signals to be distributed over tens of km. As the system performance is limited by the out-of-loop measurement noise, further improvements are possible.

[1] W. H. Oskay *et al.*, Phys. Rev. Lett. **97**, 020801 (2006).
[2] M. M. Boyd *et al.*, Phys. Rev. Lett. **98**, 083002 (2007).
[3] S. M. Foreman *et al.*, Rev. Sci. Instrum. **78**, 021101 (2007).
[4] R. F. C. Vessot *et al.*, Phys. Rev. Lett. **45**, 2081 (1980).
[5] J. C. Bergquist, in *Frontiers in Laser Spectroscopy*, Proceedings of the International School of Physics "Enrico Fermi," Course 120, edited by T. W. Hänsch and M. Inguscio (North-Holland, Amsterdam, 1992), p. 359.
[6] L.-S. Ma *et al.*, Opt. Lett. **19**, 1777 (1994).
[7] C. Daussy *et al.*, Phys. Rev. Lett. **94**, 203904 (2005).
[8] F. Narbonneau *et al.*, Rev. Sci. Instrum. **77**, 064701 (2006).
[9] J. Ye *et al.*, J. Opt. Soc. Am. B **20**, 1459 (2003).
[10] G. Grosche *et al.*, CLEO Report No. CMKK1, 2007.
[11] A. D. Ludlow *et al.*, Phys. Rev. Lett. **96**, 033003 (2006).
[12] I. Coddington *et al.*, Nat. Photon. **1**, 283 (2007).
[13] M. Musha *et al.*, Appl. Phys. B **82**, 555 (2006).
[14] A. L. Cavalieri *et al.*, Phys. Rev. Lett. **94**, 114801 (2005).
[15] C. W. Oates *et al.*, Opt. Lett. **25**, 1603 (2000).
[16] A. D. Ludlow *et al.*, Opt. Lett. **32**, 641 (2007).
[17] S. C. Rashleigh *et al.*, Opt. Lett. **3**, 60 (1978).
[18] B. C. Young *et al.*, Phys. Rev. Lett. **82**, 3799 (1999).